

Communication

Synthesis of 3-Trifluoromethyl-5,6-dihydro-[1,2,4]triazolo Pyrazine Derivatives and Their Anti-Cancer Studies

Rajaiah Raveesha ¹, Malavalli Guruswamy Dileep Kumar ² 
and Salekoppal Boregowda Benaka Prasad ^{1,*}

¹ Department of Chemistry, School of Engineering and Technology, Jain Global Campus, Jain University, Ramanagara 562112, India; raveeshar90@gmail.com

² Department of Biotechnology, Teresian Research Foundation, University of Mysore, Mysore 570005, India; dileepkmr87@gmail.com

* Correspondence: sb.benakaprasad@jainuniversity.ac.in; Fax: +91-27577199

Received: 7 November 2020; Accepted: 27 November 2020; Published: 2 December 2020



Abstract: The synthesis of a wide variety of 3-trifluoromethyl-5,6-dihydro-[1,2,4]triazolo pyrazine derivatives, by the treatment of 3-trifluoromethyl-5,6,7,8-tetrahydro-[1,2,4]triazolo[4,3- α]pyrazine hydrochloride with an array of isocyanates in the presence of triethylamine, is reported. All the target compounds were synthesized in excellent yields under mild reaction conditions. The target molecules were effectively screened for their anti-cancer properties and the results are promising. The resultant compounds were assessed for their antiproliferative action against two human colon cancer cell lines (HCT-116 and HT-29 colon cancer cell lines). The IC₅₀ range was estimated at 6.587 to 11.10 μ M showing that compound RB7 had remarkable anticancer movement on HT-29. Additionally, it was discovered that RB7 incited the mitochondrial apoptotic pathway by up-regulating Bax and down-regulating Bcl2, eventually leading to the activation of Caspase 3 in HT-29 cells and initiation of cell death via the mitochondrial apoptotic pathway.

Keywords: pyrazine derivatives; isocyanates; anti-cancer studies; HT-29 colon cancer cell lines

1. Introduction

Cancer is a leading cause of death worldwide, it is therefore urgent for medical researchers to discover efficient drugs for this disease [1]. Pyrazines, an important class of six-membered nitrogen-based heterocycles, are well known for their utility in rational drug design [2]. Ligands encompassing a pyrazine ring have been well studied and their p-donor properties have shown to be promising [3]. Pyrazine has generated great attention due to the diazine rings which form an elegant class of molecular entities, widely occurring in natural and synthetic compounds [4]. This novel unit is found in a wide variety of promising drugs pertaining to diversified therapeutic applications, namely in antidepressant [5], antipsychotic [6], antihistamine [7], anti-fungal [8], anticancer [9], antioxidant [10], and anti-inflammatory [11], etc. drugs. Structural modification with respect to substitution patterns towards the pyrazine moiety, leads to appreciable differences in the bio-active properties towards the target molecules. Therefore, continuous efforts have been undertaken to synthesize a diverse class of pyrazine derivatives which are hoped to be useful in the fight against cancer cells [12]. It is important to mention here that uncontrolled cancer cells can spread and invade different parts of the body through the blood vessels or lymphatic framework. The body is comprised of numerous sorts of cells which are important units of life and these cells develop and isolate in a limited manner to keep the body functioning normally. Tumor growth is a major clinical issue globally and it

is one of the primary reasons for mortality. Commonly occurring compounds are routinely used for anticancer medication in human cancer growth [13]. Pyrazine derivatives are known for their significant action against various human tumors. Through tubulin polymerization, the anticancer action of various subordinates of pyrazine has been accounted for in the previous report. Since various derivatives of pyrazine molecules are well reported for their anti-cancer properties, we envisioned that 3-trifluoromethyl-5,6-dihydro-[1,2,4]triazolo pyrazine derivatives (RB1-9) may exhibit interesting bio-active properties. In the literature, we could not find any report for the utilization of pyrazine derivatives (RB1-9) towards anti-cancer studies, which enthralled us to screen them for up-regulation of BAX and down-regulation of Bcl2 in HT-29 colon cancer cell lines.

2. Results and Discussion

2.1. Chemical Section

Though various reports are available in the literature for the synthesis of pyrazine derivatives (RB), there is no method available to access them under mild reaction conditions with an excellent yield, which inspired us to focus our efforts in this direction. In order to execute our idea, we have treated 3-trifluoromethyl-5,6,7,8-tetrahydro-[1,2,4]triazolo[4,3- α]pyrazine hydrochloride with 1-chloromethyl-4-iso-cyanato benzene under the catalytic influence of Et₃N in DCM at room temperature, over a period of 5 h. This produced the anticipated product in a 92% yield (Scheme 1). The structure of the molecule was confirmed by ¹H-NMR, IR, and LCMS analyses. Encouraged by this result, we treated a wide variety of isocyanates derivatives under the aforementioned condition, smoothly affording the desired compounds RB1 to RB9 in excellent yields. It is important to mention here, that all the target molecules were synthesized under mild reaction conditions with excellent reaction conversions, which is very interesting. The results are summarized in Figure 1.

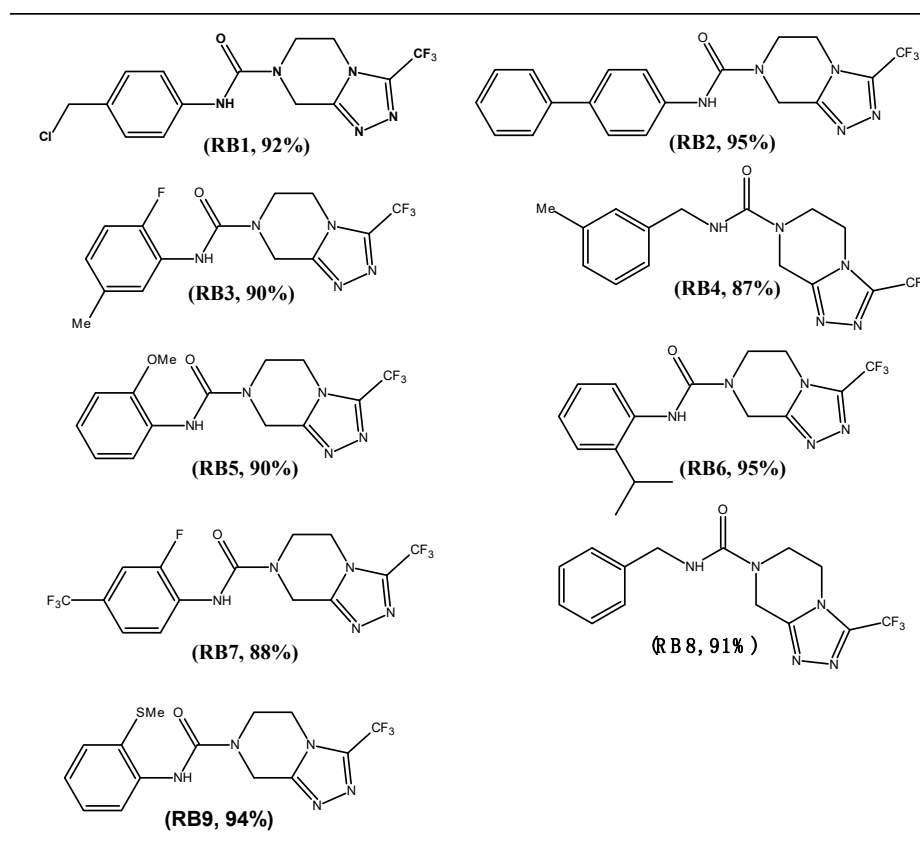
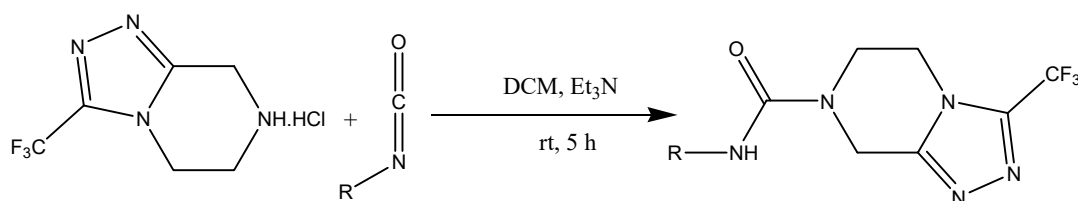


Figure 1. Synthesis of 3-trifluoromethyl-5,6-dihydro-[1,2,4]triazolo pyrazine derivatives.



Scheme 1. Synthesis of pyrazine derivatives by isocyanates series.

All reactions were carried out using 1 mmol of 3-trifluoromethyl-5,6,7,8-tetrahydro-[1,2,4]triazolo[4,3- α]pyrazine hydrochloride with isocyanates (1.2 mmol) and triethylamine (1.5 mmol) in DCM (10 mL) at RT for 5 h.

2.2. General Procedure for the Synthesis of Pyrazine Derivatives (RB1–RB9)

Triethylamine (1.5 mmol) was added to a suspension of 3-trifluoromethyl-5,6,7,8-tetrahydro-[1,2,4]triazolo[4,3- α]pyrazine hydrochloride (1 mmol) in DCM (dichloro methane) (10 mL) in RT (retention time), followed by the addition of isocyanates (1.2 mmol). The reaction mixture was stirred at room temperature for 5 h and the progress of the reaction was monitored by TLC (Thin layer chromatography). Upon completion of the reaction, the solvent was removed under reduced pressure and the residue obtained was added to water and extracted with ethyl acetate. The organic layer was washed with a brine solution and dried over anhydrous Na_2SO_4 . The solvent was evaporated and the crude product was purified by column chromatography over silica gel using chloroform: methanol (9:1) as an eluent to afford the anticipated products (RB1–RB9) (Supplementary Materials).

N-[4-(chloromethyl)phenyl]-3-(trifluoromethyl)-5,6-dihydro-[1,2,4]triazolo[4,3- α]pyrazine-7(8H)-carboxamide (RB1): (92%, off-white solid), m.p 178.8–183.6 °C $^1\text{H-NMR}$ (CDCl_3 , 400 MHz) δ : 4.00 (t, 2H, $J = 5.6$ Hz), 4.21 (t, 2H, $J = 5.2$ Hz), 4.46 (d, 2H, $J = 5.6$ Hz), 4.88 (s, 2H), 5.66 (d, 1H, $J = 4.8$ Hz), 7.28–7.32 (m, 4H). LCMS for $\text{C}_{14}\text{H}_{13}\text{ClF}_3\text{N}_5\text{O}$ (ESI + ion): $m/z = 360$ $[\text{M} + \text{H}]^+$. IR (KBr, cm^{-1}): 3356.2, 1736, 1621, 1041.

N-[3-methyl-(1,11-biphenyl)-4-yl]-3-(trifluoromethyl)-5,6-dihydro-[1,2,4]triazolo[4,3- α]pyrazine-7(8H)-carboxamide (RB2): (95%, off-white-solid), 188.6–205.9 °C, $^1\text{H-NMR}$ (CDCl_3 , 400 MHz) δ : 4.07 (t, 2H, $J = 5.6$ Hz), 4.27 (t, 2H, $J = 5.6$ Hz), 5.02 (s, 2H), 6.90–7.58 (m, 10H). LCMS for $\text{C}_{19}\text{H}_{16}\text{F}_3\text{N}_5\text{O}$ MS (ESI + ion): $m/z = 388$ $[\text{M} + \text{H}]^+$. IR (KBr, cm^{-1}): 3429, 3030, 1654, 1283, 1078, 981.

N-(2-fluoro-5-methylphenyl)-3-(trifluoromethyl)-5,6-dihydro-[1,2,4]triazolo[4,3- α]pyrazine-7(8H)-carboxamide (RB3): (90%, off-white-solid), 196.7–201.7 °C, $^1\text{H-NMR}$ (CDCl_3 , 400 MHz) δ : 2.32 (s, 3H), 4.05 (t, 2H, $J = 6$ Hz), 4.27 (t, 2H, $J = 4.8$ Hz), 4.99 (s, 2H), 6.78–7.76 (m, 4H) LCMS for $\text{C}_{14}\text{H}_{13}\text{F}_4\text{N}_5\text{O}$ MS (ESI + ion): $m/z = 344$ $[\text{M} + \text{H}]^+$. IR (KBr, cm^{-1}): 3240, 2926, 1638, 1498, 1042, 939, 871.

N-(3-methylbenzene)-3-(trifluoromethyl)-5,6-dihydro-[1,2,4]triazolo[4,3- α]pyrazine-7(8H)-carboxamide (RB4): (87%, white-solid), 178.3, 185.1 °C, $^1\text{H-NMR}$ (CDCl_3 , 400 MHz) δ : 2.35 (d, 2H, $J = 8$ Hz), 3.99 (t, 2H, $J = 6.8$ Hz), 4.20 (t, 2H, $J = 6.8$ Hz), 4.43 (d, 2H, $J = 7.2$ Hz), 4.84 (s, 2H), 5.22 (s, 1H), 7.11–7.28 (m, 3H). LCMS for $\text{C}_{15}\text{H}_{16}\text{F}_3\text{N}_5\text{O}$ MS (ESI + ion): $m/z = 341$ $[\text{M} + \text{H}]^+$. IR (KBr, cm^{-1}): 3354, 2919, 1629, 1535, 1498, 1138, 1011, 947.

N-(2-methoxyphenyl)-3-(trifluoromethyl)-5,6-dihydro-[1,2,4]triazolo[4,3- α]pyrazine-7(8H)-carboxamide (RB5): (90%, white-solid), 142.4, 149.9 °C, $^1\text{H-NMR}$ (CDCl_3 , 400 MHz) δ : 2.43 (s, 3H), 4.09 (t, 2H, $J = 5.6$ Hz), 4.29 (t, 2H, $J = 5.2$ Hz), 5.06 (s, 2H), 7.06–8.11 (m, 5H). LCMS for $\text{C}_{14}\text{H}_{14}\text{F}_3\text{N}_5\text{O}_2$ MS (ESI + ion): $m/z = 342$ $[\text{M} + \text{H}]^+$. IR (KBr, cm^{-1}): 3309, 2962, 1662, 1600, 1389, 1012, 939, 747.

N-(2-isopropylphenyl)-3-(trifluoromethyl)-5,6-dihydro-[1,2,4]triazolo[4,3- α]pyrazine-7(8H)-carboxamide (RB6): (95%, Off-white-solid), 168.1–172.9 °C. $^1\text{H-NMR}$ (CDCl_3 , 400 MHz) δ : 1.26 (d, 6H, $J = 6.8$ Hz), 3.05 (t, 1H, $J = 6.8$ Hz), 4.02 (t, 2H, $J = 5.6$ Hz), 4.23 (t, 3H, $J = 5.2$ Hz), 4.92 (s, 2H), 6.44–7.42 (m, 5H).

LCMS for $C_{16}H_{18}F_3N_5O$ MS (ESI + ion): $m/z = 355 [M + H]^+$. IR (KBr, cm^{-1}): 3290, 2958, 1636, 1521, 1389, 1246, 1122, 1032, 940.

N-(2-fluoro-4-trifluoromethylphenyl)-3-(trifluoromethyl)-5,6-dihydro-[1,2,4]triazolo[4,3- α]pyrazine-7(8H)-carboxamide (RB7): (88%, off-white-solid), 171.4–176.4 °C, 1H -NMR ($CDCl_3$, 400 MHz) δ : 4.10 (t, 2H, $J = 7.6$ Hz), 4.31 (t, 2H, $J = 6.8$ Hz), 5.04 (d, 2H, $J = 12$ Hz), 6.94–8.41 (m, 4H). LCMS for $C_{14}H_{10}Cl_2F_7N_5O$ MS (ESI + ion): $m/z = 398 [M + H]^+$. IR (KBr, cm^{-1}): 3342, 646, 1501, 1335, 1277, 1121, 1014, 894.

N-(benzyl)-3-(trifluoromethyl)-5,6-dihydro-[1,2,4]triazolo[4,3- α]pyrazine-7(8H)-carboxamide (RB8): (96%, white-solid), 194.4–199.3 °C. 1H -NMR ($CDCl_3$, 400 MHz) δ : 3.99 (t, 2H, $J = 5.6$ Hz), 4.20 (t, 2H, $J = 5.2$ Hz), 4.48 (d, 2H, $J = 5.6$ Hz), 5.39 (s, 1H), 7.28–7.36 (m, 5H). LCMS for $C_{14}H_{14}F_3N_5O$ MS (ESI + ion): $m/z = 326 [M + H]^+$. IR (KBr, cm^{-1}): 3325, 2924, 1626, 1543, 1280, 1046, 938.

N-[2-(methylthio)phenyl]-3-(trifluoromethyl)-5,6-dihydro-[1,2,4]triazolo[4,3- α]pyrazine-7(8H)-carboxamide (RB9): (94%, off-white-solid), 191.9–197.3 °C. 1H -NMR ($CDCl_3$, 400 MHz) δ : 2.41 (d, 3H, $J = 10.8$ Hz), 4.08 (t, 2H, $J = 7.6$ Hz), 4.29 (t, 2H, $J = 6.8$ Hz), 5.04 (s, 2H), 7.05–8.10 (m, 5H). LCMS for $C_{14}H_{14}F_3N_5O_5$ MS (ESI + ion): $m/z = 358 [M + H]^+$. IR (KBr, cm^{-1}): 3299, 2930, 1644, 1398, 1039, 943.

2.3. Biological Studies

The cytotoxic examination and acridine orange and ethidium bromide assay

By MTT assay, resultant compounds were examined for in vitro cytotoxic action in human colon cancer cell lines such as HT-29 and HCT-116. Reduced forms of formazan crystals were obtained from MTT—a tetrazolium salt. The viability of cells was directly measured by the intensity of the formation of formazan. The IC_{50} estimation of 8.18 μM concentration reveals that the R7 compound shows antitumor activity (Table 1 and Figure 2a,b). Acridine orange is a vital dye that recolors live, as well as dead cells. A given sample treated with cells in various concentrations showed a remarkable growth in apoptosis. The report revealed that samples with cell membrane injury were caused due to early apoptosis at 8.18 μM treatment (Figure 2c).

Table 1. IC_{50} for Pyrazine derivatives.

Compounds	HCT-116	HT-29	Chang Liver (Normal Cells)
RB1	23.25 \pm 0.8	28.32 \pm 0.5	>100
RB2	32.21 \pm 0.6	29.23 \pm 0.6	>50
RB3	28.32 \pm 1.2	33.17 \pm 1.2	>100
RB4	45.23 \pm 0.23	38.26 \pm 0.45	>100
RB5	52.32 \pm 0.7	32.16 \pm 0.78	>50
RB6	22.36 \pm 0.65	25.23 \pm 0.95	>100
RB7	15.23 \pm 0.9	8.18 \pm 1.2	>100
RB8	25.23 \pm 1.4	19.36 \pm 1.23	>50
RB9	22.56 \pm 1.12	18.65 \pm 0.89	>100
Cisplatin	6.15 \pm 1.4	5.23 \pm 0.91	>50

IC_{50} values were expressed in triplicate experiments from 0.7 to 200 micro molar and IC_{50} values were calculated using prism pad 5.0.

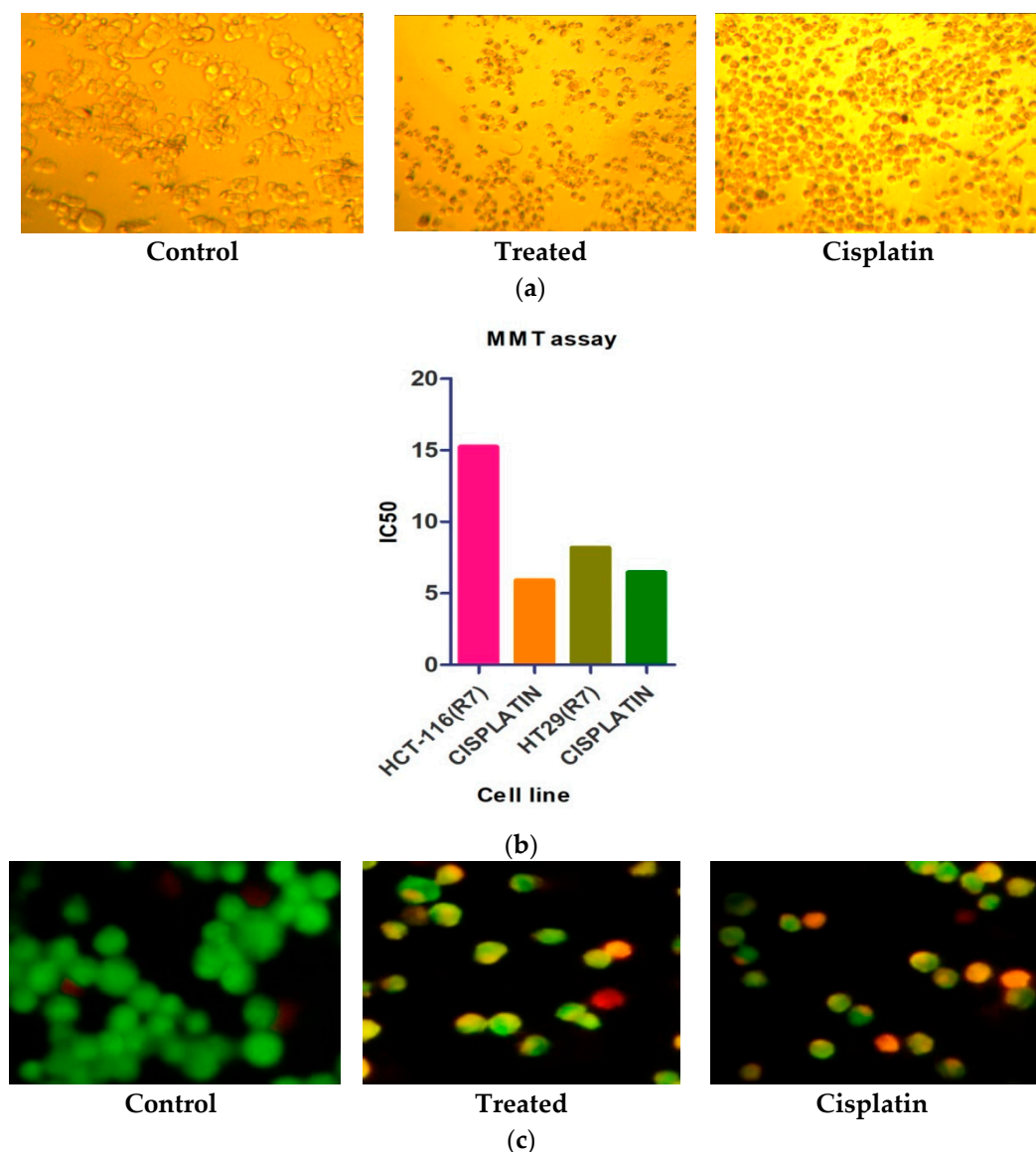


Figure 2. (a) The morphological changes in HT-29 cells in control, treated and cisplatin with specified concentration was observed and visualized under light microscope. (b) the IC₅₀ of RB-7 on different human cancer cell lines along with cisplatin as a standard drug. (c) Apoptosis inducing-activity of RB7 by AO/EB staining for specific cell line HT-29 in RB7 with 8.18 μ M concentration.

2.4. Up-Regulation of BAX and Down-Regulation of Bcl2 in HT-29 Cell Lines

The apoptosis process is a quick and irreversible procedure to effectively dispense with inadequate cells. The evasion of apoptosis by threatening cells is a sign of malignant growth. For malignant growth advancement, apoptosis can be viewed as a significant obstruction, maintaining a strategic distance from apoptosis is essential to tumor improvement and protection from treatment. The inborn apoptotic pathway is controlled and managed by the Bcl2 family proteins [14]. The Bcl2 family proteins are known to be significant watchmen of apoptotic reactions. The commencement of apoptosis was observed to rely on the harmony between a professional apoptotic and hostility to an apoptotic protein that intercedes cell death and development.

In numerous malignant growth types, the anti-apoptotic protein Bcl2 may assume an important role. The over articulation of Bcl2 in numerous malignant growths may restrain the prop-apoptotic signals which permit cancer cells to undergo death. The counter apoptotic Bcl2 forestalls apoptosis either by forestalling the arrival of mitochondrial apoptosome factors, for example, cytochrome c

and Apaf1 into the cytoplasm or by sequestering preforms of death-driving cysteine proteases called caspases. Cells become delicate to apoptosis when the degree of apoptotic protein BAX is up-regulated. An elevated level of master apoptosis protein Bax sharpens the cells for apoptosis. The pro-apoptotic protein Bax triggers the initiation of caspase 3 by inciting the arrival of mitochondrial cytochrome C and AIF into the cytoplasm by means of changes in the pores, subsequently prompting caspase 3 activation [15]. In the current investigation, d1 inhibited the activation of Bcl-2 mRNA articulation and expanded the up-regulation of Bax. After the successful synthesis of pyrazine derivatives (RB1–9), we utilized them for anti-cancer studies. Results revealed that d1 expanded Bax transcripts and hindered Bcl2 transcripts in HT-29 cells (Figure 3) and revealed a logical increment in caspase 3 inception when contrasted with controls (Figure 3), proposing that d1 causes cell death through a mitochondrial apoptotic pathway.

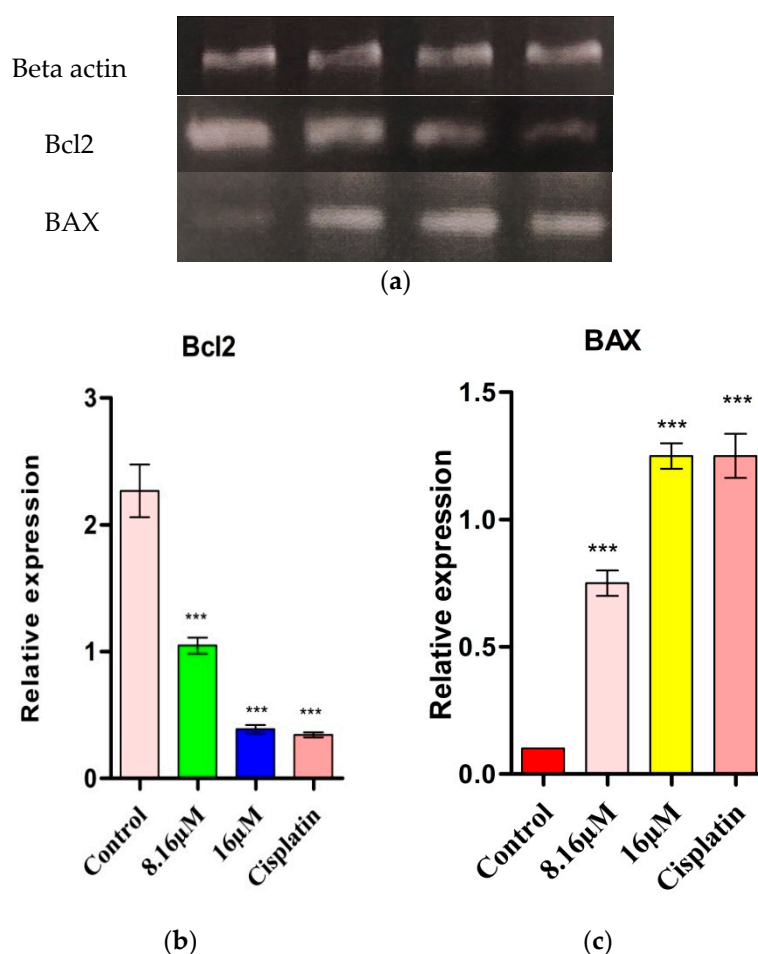


Figure 3. (a) The relative gene expression of BAX in treated HT-29 along with the control and cisplatin. (b) The relative gene expression of Bcl2 in treated HT-29 along with the control and cisplatin. (c) The relative gene expression of Bax in treated HT-29 along with the control and positive drug cisplatin. Statistical significance is expressed as *** $p < 0.0001$ by using one-way ANOVA.

The apoptosis process is a quick and irreversible procedure to effectively dispense with inadequate cells. The evasion of apoptosis by threatening cells is a sign of malignant growth. For malignant growth advancement, apoptosis can be viewed as a significant obstruction, and maintaining a strategic distance from apoptosis is essential to tumor improvement and protection from treatment. The inborn apoptotic pathway is controlled and managed by the Bcl-2 family proteins [14]. The Bcl-2 family proteins are known to be significant watchmen of the apoptotic reaction. It was observed that the

commencement of apoptosis relies upon the harmony between a professional apoptotic and hostility to the apoptotic protein that intercedes cell death and development.

In numerous malignant growth types, the anti-apoptotic protein Bcl2 may assume an important role. The over articulation of Bcl2 in numerous malignant growths may restrain the pro-apoptotic signals which permit cancer cells to undergo death. The counter apoptotic Bcl2 forestalls apoptosis, either by forestalling the arrival of mitochondrial apoptosome factors, for example, cytochrome c and Apaf1 into the cytoplasm or by sequestering preforms of death-driving cysteine proteases called caspases. Cells become delicate to apoptosis when the degree of genius apoptotic protein BAX is up-regulated. An elevated level of master apoptosis protein Bax sharpens the cells for apoptosis. The pro-apoptotic protein Bax triggers the initiation of caspase 3 by inciting the arrival of mitochondrial cytochrome C and AIF into the cytoplasm by means of changes in the pores, subsequently prompting caspase 3 activation [15]. In the current investigation, d1 inhibits the activation of Bcl2 mRNA articulation and expanded the up-regulation of Bax. After the successful synthesis of pyrazine derivatives (RB1-9), we utilized them for anti-cancer studies. The results revealed that d1 expanded Bax transcripts and hindered Bcl2 transcripts in HT-29 cells (Figure 3) and revealed a logical increment in caspase 3 inception when contrasted with the control (Figure 3), proposing that d1 causes cell death through a mitochondrial apoptotic pathway.

3. Materials and Methods

3.1. Chemicals and Cell Lines

We purchased MTT [3-(4,5-dimethylthiazol-2-yl)-2,5-diphenyl tetrazolium bromide] from Sigma Chemicals. We obtained human HT-29 development cell lines—HT-29 and HCT-116 from the National Centre for Cell Science, Pune, India. Cells developed in an ideal media magnified with 10% warmth inactivated fetal bovine serum (FBS), 100 µg of streptomycin/mL, 100 U/mL of penicillin, and were incubated in humidified environment with 5% CO₂ at 37 °C.

3.2. Statistical Analysis

Statistical analysis was accomplished by one-way and one-way ANOVA conveyed by Bonferroni's multiple comparison test. This was used to examine the correlation $p < 0.05$ and was used to signify statistical significance when computing the IC₅₀ of all the compounds. Data were analyzed utilizing Graph Pad Prism 5.0 software.

3.3. MTT Cell Viability Assay

Cytotoxic activity of chalcones was examined by applying the MTT assay [16]. In 100 µL DMEM 1×10^4 cells/well had seeded. A total of 10% FBS (fetal bovine serum) was magnified in all wells of a 96-well micro culture plate and incubated at 37 °C in CO₂, followed by 48 h of incubation. A total of 10 µL MTT [3-(4,5-dimethylthiazol-2-yl)-2,5-diphenyl tetrazolium bromide] (5 mg mL^{-1}) was added to all wells, and the plates further incubated for 4 h. From the supernatant of each well in 100 µL of DMSO, the crystals of formazan were taken up and absorbance was recorded at 540 nm.

3.4. Acridine Orange/Ethidium Bromide Staining

Through the AO/EB (acridine orange and ethidium bromide) double staining method, nuclear recoloring was executed [16]. HT-29 cells were collected from the control and d1 treated category. In a fixative arrangement (methanol: acidic corrosive (3:1)) cells were fixed and spread on clean glass slides, the slides were hydrated with PBS, and recolored by acridine orange/ethidium bromide (1:1). The cells were washed thoroughly by using PBS and detected through fluorescent instruments at 400–500 nm.

3.5. RT-PCR

RT-PCR was performed to analyze β -Actin RNA articulation, BAX, Bcl2, and caspase 3 by the Techno Prime framework. As per the manufacturer's instruction, cDNA was synthesized from 2 μ g of RNA utilizing a verso cDNA synthesis kit, accompanied by an oligo dT primer. The reaction volume was set to 20 μ L and synthesis of cDNA was carried out for 1 h at 42 °C, followed by RT inactivation for 5 min at 85 °C. Samples of the resultant products were examined in 1.5% agarose gel [16].

4. Conclusions

We have successfully developed an efficient protocol for the synthesis of a wide variety of 3-trifluoromethyl-5,6-dihydro-[1,2,4]triazolo pyrazine derivatives in excellent yields, under mild reaction conditions. All the synthesized compounds were thoroughly characterized using ¹H-NMR, IR, and LC-MS analyses. All the synthesized compounds were then utilized for anti-cancer studies. The up-regulation of Bax has expansive applications for the enlistment of apoptosis in disease treatment. Overexpression of the Bax protein prompts the arrival of cytochrome C, initiation of the caspase pathway in compound RB7, and actuates apoptosis in HT-29 cells, ultimately leading to activation of the mitochondrial apoptotic pathway and cell death.

Supplementary Materials: The following are available online. Figure S1: RB1 FT-IR, LC-MS and ¹H-NMR, Figure S2: RB2-FT-IR, LC-MS and ¹H-NMR, Figure S3: RB3-FT-IR, LC-MS and ¹H-NMR, Figure S4: RB4- FT-IR, LC-MS and ¹H-NMR, Figure S5: RB5-FT-IR, LC-MS and ¹H-NMR, Figure S6: RB6 FT-IR, LC-MS and ¹H-NMR, Figure S7: RB7 -FT-IR, LC-MS and ¹H-NMR, Figure S8: RB8 -FT-IR, LC-MS and ¹H-NMR, Figure S9: RB9-FT-IR, LC-MS and ¹H-NMR.

Author Contributions: Synthesis and characterization were carried out by R.R., writing the research paper, editing, and biological activity experiments, and their interpretation were carried out by M.G.D.K., the research supervisor is S.B.B.P. All authors have read and agreed to the published version of the manuscript.

Funding: No external fund was received during this research.

Acknowledgments: The authors thank the Department of Basic Science and Technology, Jain University for the financial support given for this research work and their constant support in encouraging this research work.

Conflicts of Interest: Authors declare no potential conflict of interest.

References

1. Patridge, E.; Gareiss, P.; Kinch, M.S.; Hoyer, D. An analysis of FDA-approved drugs: Natural products and their derivatives. *Drug Discov. Today* **2016**, *21*, 204–207. [[CrossRef](#)] [[PubMed](#)]
2. Podraza, K.F. Synthesis and thermal rearrangement of allylic 3,5,6-trimethyl-2-pyrazinylacetates: A heterocyclic carroll rearrangement. *J. Heterocycl. Chem.* **1986**, *23*, 581–583. [[CrossRef](#)]
3. Gao, J.; Luo, X.; Li, Y.; Gao, R.; Chen, H.; Ji, D. Synthesis and biological evaluation of 2-oxo-pyrazine-3-carboxamide-yl nucleoside analogues and their epimers as inhibitors of influenza A viruses. *Chem. Biol. Drug Des.* **2015**, *85*, 245. [[CrossRef](#)]
4. Liu, W.; Tang, Y.; Guo, Y.; Sun, B.; Zhu, H.; Xiao, Y.; Dong, D.; Yang, C. Synthesis, characterization and bioactivity determination of ferrocenyl urea derivatives. *Appl. Organometal. Chem.* **2012**, *26*, 189–193. [[CrossRef](#)]
5. Li, H.Q.; Lv, P.C.; Yan, T.o.; Zhu, H.L. Urea derivatives as anticancer agents. *Anti-Cancer Agents Med. Chem.* **2009**, *9*, 471–480. [[CrossRef](#)]
6. El-Kashef, H.S.; El-Emary, T.I.; Gasquet, M.; Timon-David, P.; Maldonado, J.; Vanelle, P. New pyrazolo [3, 4-b] pyrazines: Synthesis and biological activity. *Die Pharm.* **2000**, *55*, 572.
7. Moree, W.J.; Li, B.F.; Jovic, F.; Coon, T.; Yu, J.; Gross, R.S.; Tucci, F.; Marinkovic, D.; Zamani-Kord, S.; Malany, S.; et al. Characterization of novel selective H1-antihistamines for clinical evaluation in the treatment of insomnia. *J. Med. Chem.* **2009**, *52*, 5307–5310. [[CrossRef](#)]
8. Goetz, M.A.; Zhang, C.; Zink, D.L.; Arocho, M.; Vicente, F.; Bills, G.F.; Polishook, J.; Dorso, K.; Onishi, R.; Gill, C.; et al. Coelomycin, a highly substituted 2,6-dioxo-pyrazine fungal metabolite antibacterial agent discovered by Staphylococcus aureus fitness test profiling. *J. Antibiot.* **2010**, *63*, 512–518. [[CrossRef](#)] [[PubMed](#)]

9. Mannam, M.R.; Devineni, S.R.; Pavuluri, C.M.; Chamarthi, N.R.; Kottapalli, R.S. Urea and thiourea derivatives of 3-trifluoromethyl-5,6,7,8-tetrahydro-[1,2,4]triazolo[4,3- α]pyrazine: Synthesis, characterization, antimicrobial activity and docking studies. *Phosphorus Sulfur Silicon Relat. Elem.* **2019**, *194*, 922–932. [[CrossRef](#)]
10. Ser, H.L.; Palanisamy, U.D.; Yin, W.F.; Abd Malek, S.N.; Chan, K.G.; Goh, B.H.; Lee, L.H. Presence of antioxidative agent, Pyrrolo [1,2-a] pyrazine-1,4-dione, hexahydro-in newly isolated *Streptomyces mangrovisoli* sp. nov. *Front. Microbiol.* **2015**, *6*, 854. [[CrossRef](#)]
11. Opletalová, V.; Patel, A.; Boulton, M.; Dundrová, A.; Lacinová, E.; Převorová, M.; Appeltauerová, M.; Coufalová, M. 5-Alkyl-2-pyrazinecarboxamides, 5-alkyl-2-pyrazinecarbonitriles and 5-alkyl-2-acetylpyrazines as synthetic intermediates for antiinflammatory agents. *Collect. Czechoslov. Chem. Commun.* **1996**, *61*, 1093–1101. [[CrossRef](#)]
12. Temple, C., Jr.; Wheeler, G.P.; Elliott, R.D.; Rose, J.D.; Kussner, C.L.; Comber, R.N.; Montgomery, J.A. New anticancer agents: Synthesis of 1,2-dihydropyrido [3,4-b]pyrazines(1-deaza-7,8-dihydropteridines). *J. Med. Chem.* **1982**, *25*, 1045–1050. [[CrossRef](#)]
13. Kassis, P.; Brzeszcz, J.; Bénétiau, V.; Lozach, O.; Meijer, L.; Le Guével, R.; Guillouzo, C.; Lewiński, K.; Bourg, S.; Colliandre, L.; et al. Synthesis and biological evaluation of new 3-(6-hydroxyindol-2-yl)-5-(Phenyl) pyridine or pyrazine V-Shaped molecules as kinase inhibitors and cytotoxic agents. *Eur. J. Med. Chem.* **2011**, *46*, 5416–5434. [[CrossRef](#)]
14. Naseri, M.H.; Mahdavi, M.; Davoodi, J.; Tackallou, S.H.; Goudarzvand, M.; Neishabouri, S.H. Up-regulation of Bax and down-regulation of Bcl2 during 3-NC mediated apoptosis in human cancer cells. *Cancer Cell Int.* **2015**, *15*, 55. [[CrossRef](#)]
15. Green, D.R.; Reed, J.C. Mitochondria and apoptosis. *Science* **1998**, *5381*, 1309–1312. [[CrossRef](#)]
16. Guruswamy, D.K.; Jayarama, S. Proapoptotic and anti-angiogenic activity of (2E)-3-(2-bromo-6-hydroxy-4-methoxyphenyl)-1-(naphthalene-2-yl) prop-2-en-1-one in MCF7 cell line. *Chem. Pap.* **2020**, *74*, 2229–2237. [[CrossRef](#)]

Publisher's Note: MDPI stays neutral with regard to jurisdictional claims in published maps and institutional affiliations.



© 2020 by the authors. Licensee MDPI, Basel, Switzerland. This article is an open access article distributed under the terms and conditions of the Creative Commons Attribution (CC BY) license (<http://creativecommons.org/licenses/by/4.0/>).